J Physiol 591.17 (2013) pp 4223–4235

The Journal of Physiology

Aldosterone increases cardiac vagal tone via G protein-coupled oestrogen receptor activation

G. Cristina Brailoiu[1], Khalid Benamar[2], Jeffrey B. Arterburn[3], Erhe Gao[4], Joseph E. Rabinowitz[4,5], Walter J. Koch[4,5] and Eugen Brailoiu[4,5]

[1]*Department of Pharmaceutical Sciences, Thomas Jefferson University, Jefferson School of Pharmacy, Philadelphia, PA 19107, USA*
[2]*Center for Substance Abuse Research,* [4]*Center for Translational Medicine and* [5]*Department of Pharmacology, Temple University School of Medicine, Philadelphia, PA 19140, USA*
[3]*Department of Chemistry and Biochemistry, New Mexico State University, Las Cruces, NM 88003, USA*

Key points

- Faster cellular effects of aldosterone incompatible with the genomic effects mediated by mineralocorticoid receptors have been proposed for 40 years but the receptors remained elusive.
- Recently, aldosterone has been shown to activate the G protein-coupled oestrogen receptor (GPER) in the vasculature.
- Our results indicate that aldosterone activates the GPER in cardiac vagal neurons of nucleus ambiguus leading to an increase in cytosolic Ca^{2+} concentration and depolarization; in addition, *in vivo* studies indicate that microinjection of aldosterone in nucleus ambiguus produces bradycardia in conscious rats.
- In summary, our results identified a new role for aldosterone in the modulation of cardiac vagal tone via GPER activation in nucleus ambiguus.

Abstract In addition to acting on mineralocorticoid receptors, aldosterone has been recently shown to activate the G protein-coupled oestrogen receptor (GPER) in vascular cells. In light of the newly identified role for GPER in vagal cardiac control, we examined whether or not aldosterone activates GPER in rat nucleus ambiguus. Aldosterone produced a dose-dependent increase in cytosolic Ca^{2+} concentration in retrogradely labelled cardiac vagal neurons of nucleus ambiguus; the response was abolished by pretreatment with the GPER antagonist G-36, but was not affected by the mineralocorticoid receptor antagonists, spironolactone and eplerenone. In Ca^{2+}-free saline, the response to aldosterone was insensitive to blockade of the Ca^{2+} release from lysosomes, while it was reduced by blocking the Ca^{2+} release via ryanodine receptors and abolished by blocking the IP_3 receptors. Aldosterone induced Ca^{2+} influx via P/Q-type Ca^{2+} channels, but not via L-type and N-type Ca^{2+} channels. Aldosterone induced depolarization of cardiac vagal neurons of nucleus ambiguus that was sensitive to antagonism of GPER but not of mineralocorticoid receptor. *in vivo* studies, using telemetric measurement of heart rate, indicate that microinjection of aldosterone into the nucleus ambiguus produced a dose-dependent bradycardia in conscious, freely moving rats. Aldosterone-induced bradycardia was blocked by the GPER antagonist, but not by the mineralocorticoid receptor antagonists. In summary, we report for the first time that aldosterone decreases heart rate by activating GPER in cardiac vagal neurons of nucleus ambiguus.

(Received 18 April 2013; accepted after revision 19 July 2013; first published online 22 July 2013)
Corresponding author E. Brailoiu: Center for Translational Medicine, Temple University School of Medicine, MERB, 3500 N. Broad Street, Philadelphia, PA 19140, USA. Email: ebrailou@temple.edu

Abbreviations 2-APB, 2-aminoethoxydiphenyl borate; $[Ca^{2+}]_i$, cytosolic Ca^{2+} concentration; GPER, G protein-coupled oestrogen receptor; HBSS, Hanks' balanced salt solution; IP_3, inositol 1,4,5-trisphosphate.

© 2013 The Authors. The Journal of Physiology © 2013 The Physiological Society

DOI: 10.1113/jphysiol.2013.257204

Introduction

Aldosterone, a member of the renin–angiotensin–aldosterone system, is classically involved in the regulation of salt and water homeostasis by acting on mineralocorticoid receptors in the kidney. Activation of mineralocorticoid receptors by aldosterone leads to genomic effects, modulation of gene transcription and protein synthesis, characterized by a delayed onset of action. Faster actions of aldosterone, insensitive to blockade of mineralocorticoid receptors, have been described *in vitro* and *in vivo* (Schneider *et al.* 1997; Wehling *et al.* 1998; Liu *et al.* 2003; Schmidt *et al.* 2003; Lösel *et al.* 2004). Moreover, rapid non-genomic aldosterone effects were reported in the mineralocorticoid receptor knockout mouse suggesting that they were produced by a receptor distinct from the intracellular mineralocorticoid receptor (Haseroth *et al.* 1999). Recently, aldosterone has been reported to act rapidly via the G protein-coupled oestrogen receptor (GPER; Gros *et al.* 2011*a*,*b*, 2013; Feldman & Gros, 2011).

In addition to the peripheral effects, aldosterone acts centrally to stimulate sympathetic tone and to increase the blood pressure (Yu *et al.* 2008; Zhang *et al.* 2008). The effects of aldosterone on vagal tone are poorly understood: aldosterone has been reported to increase (Heindl *et al.* 2006), decrease (Yee & Struthers, 1998; Schmidt *et al.* 2005) or to produce biphasic (Schmidt *et al.* 1999) effects on the cardiac vagal tone and baroreflex. As we recently identified that activation of GPER in the nucleus ambiguus increases vagal tone and produces bradycardia (Brailoiu *et al.* 2013), in the current study we examined the *in vitro* and *in vivo* effects of aldosterone mediated by GPER in cardiac preganglionic neurons of nucleus ambiguus.

Methods

Ethical approval

Animal protocols were approved by the Institutional Animal Care and Use Committee of Thomas Jefferson University and Temple University.

Chemicals

Aldosterone, 2-aminoethoxydiphenyl borate (2-APB), spironolactone, ω-conotoxin MVIIC and ω-conotoxin GVIA were from Sigma-Aldrich (St Louis, MO, USA); eplerenone was from Tocris Bioscience (R&D Systems, Minneapolis, MN, USA); xestospongin C and ryanodine were from EMD Chemicals Inc. (San Diego, CA, USA); and G-1 and G-36 were synthesized by J. B. Arterburn.

Animals

Neonatal Sprague–Dawley rats (1–2 days old) were used for retrograde tracing, and neuronal culture. Adult male Sprague–Dawley rats (200–250 g) were used for telemetry experiments. At the end of the experiments, anesthetized adult rats were euthanized by CO_2 inhalation followed by decapitation.

Neuronal labelling and culture

Cardiac vagal preganglionic neurons of nucleus ambiguus were retrogradely labelled by intrapericardial injection of rhodamine (X-RITC, 40 μl, 0.01%, Invitrogen, Carlsbad, CA, USA), as previously described (Brailoiu *et al.* 2012, 2013). Medullary neurons were dissociated and cultured, 24 h after rhodamine injection. Briefly, the brains were quickly removed and immersed in ice-cold Hanks' balanced salt solution (Mediatech, Manassas, VA, USA). The ventral side of the medulla (containing nucleus ambiguus) was dissected, minced, and the cells were dissociated by enzymatic digestion with papain, followed by mechanical trituration. After centrifugation at 500 *g*, fractions enriched in neurons were collected and resuspended in culture medium containing Neurobasal-A (Invitrogen), which promotes the survival of postnatal neurons, 1% GlutaMax (Invitrogen), 2% penicillin–streptomycin–amphotericin B solution (Mediatech) and 10% fetal bovine serum (Atlanta Biologicals, Lawrenceville, GA, USA). Cells were plated on round 25 mm glass coverslips previously coated with poly-L-lysine (Sigma-Aldrich) in 6-well plates. Cultures were maintained at 37°C in a humidified atmosphere with 5% CO_2. The mitotic inhibitor cytosine β-arabino furanoside (1 μM; Sigma-Aldrich) was added to the culture to inhibit glial cell proliferation (Schöniger *et al.* 2001). Cells were used for calcium imaging after 2–4 days in culture.

Calcium imaging

Measurements of $[Ca^{2+}]_i$ were carried out in rhodamine-labelled neurons as previously described (Brailoiu *et al.* 2012, 2013). Cells were incubated with the acetoxymethyl ester form of fura-2 (fura-2 AM; 4 μM; Invitrogen) in Hanks' balanced salt solution (HBSS) at room temperature for 45 min, in the dark, washed three times with dye-free HBSS, and then incubated for another 45 min to allow for complete de-esterification of the dye. Coverslips (25 mm diameter) were subsequently mounted in an open bath chamber (RP-40LP, Warner Instruments, Hamden, CT, USA) on the stage of an inverted microscope Nikon Eclipse TiE (Nikon Inc., Melville, NY, USA). The microscope was equipped with a Perfect Focus System and a Photometrics CoolSnap HQ2 CCD camera. During the experiments, the Perfect Focus System was activated. Rhodamine (emission 580 nm)-labelled neurons were identified after excitation at 510 nm. Fura-2 AM fluorescence (emission 510 nm), following alternate excitation at 340 and 380 nm, was acquired at a

© 2013 The Authors. The Journal of Physiology © 2013 The Physiological Society

frequency of 0.25 Hz. Images were acquired and analysed using NIS-Elements AR software (Nikon). The ratio of the fluorescence signals (340 nm/380 nm) was converted to Ca^{2+} concentrations (Grynkiewicz *et al.* 1985).

Measurement of membrane potential

The relative changes in membrane potential of single neurons were evaluated using bis-(1,3-dibutylbarbituric acid) trimethine oxonol ($DiBAC_4(3)$; Invitrogen), a slow response voltage-sensitive dye, as previously described (Brailoiu *et al.* 2010, 2013). Upon membrane hyperpolarization, the dye concentrates in the cell membrane, leading to a decrease in fluorescence intensity, while depolarization induces the sequestration of the dye into the cytosol, resulting in an increase of the fluorescence intensity (Brauner *et al.* 1984). Cultured neurons were incubated for 30 min in HBSS containing 0.5 mM $DiBAC_4(3)$ and fluorescence monitored at 0.17 Hz (excitation/emission 480 nm/540 nm). Calibration of $DiBAC_4(3)$ fluorescence following background subtraction was performed using the Na^+–K^+ ionophore gramicidin in Na^+-free physiological solution and various concentrations of K^+ (to alter membrane potential) and *N*-methylglucamine (to maintain osmolarity; Brauner *et al.* 1984). Under these conditions the membrane potential is approximately equal to the K^+ equilibrium potential determined by the Nernst equation. The intracellular K^+ and Na^+ concentration were assumed to be 130 mM and 10 mM, respectively.

Surgical procedures

Male Sprague–Dawley rats (200–250 g) were anaesthetized with an intraperitoneal injection of a mixture of ketamine hydrochloride (100–150 mg kg^{-1}) and acepromazine maleate (0.2 mg kg^{-1}). Animals were placed into a stereotaxic instrument; a guide C315G cannula (PlasticsOne, Roanoke, VA, USA) was bilaterally inserted into the nucleus ambiguus and fixed in position with dental cement. The stereotaxic coordinates for identification of nucleus ambiguus were: 12.24 mm posterior to bregma, 2.1 mm from the midline and 8.2 mm ventral to the dura mater (Paxinos & Watson, 1998). A C315DC cannula dummy (PlasticsOne) of identical length was inserted into the guide cannula to prevent any contamination. For the implantation of transmitters, an incision 2 cm in length was made along the linea alba, and the underlying tissue was dissected and retracted. A calibrated transmitter (E-mitters, series 4000; Mini Mitter, Sunriver, OR, USA) was inserted in the intraperitoneal space, as previously described (Benamar *et al.* 2010). After the transmitter was passed through the incision, the abdominal musculature and dermis were sutured independently, and the animals were returned to individual cages. The animals were observed daily to ensure health and recovery.

Microinjection into nucleus ambiguus

One week after surgery, either vehicle, or the compound tested was bilaterally microinjected into the nucleus ambiguus, using a C315I internal cannula (33 gauge, PlasticsOne), without handling the rats. At least 2 h were allowed between two injections for recovery. In all *in vivo* experiments, two types of controls were used: microinjection of saline was used as a negative control and microinjection of L-glutamate (5 mM, 50 nl with a Neuros Hamilton syringe, Model 7000.5 KH SYR) was used for the functional identification of nucleus ambiguus (Chitravanshi *et al.* 2009; Brailoiu *et al.* 2013). In some experiments, rats bearing a cannula in nucleus ambiguus and the intraperitoneal transmitter were anaesthetized with ketamine hydrochloride (100–150 mg kg^{-1}) and acepromazine maleate (0.2 mg kg^{-1}), and one of the femoral veins was cannulated for intravenous injection of atropine.

Telemetric heart rate monitoring

The signal generated by transmitters was collected via series 4000 receivers (Mini Mitter) placed underneath the home cage. VitalView software (Mini Mitter) was used for data acquisition. Each data point represents the average heart rate per 1 min.

Statistical analysis

Data were expressed as mean ± standard error of mean (SEM). One-way ANOVA followed by *post hoc* analysis using Bonferonni and Tukey tests was used to evaluate significant differences between groups; $P < 0.05$ was considered statistically significant.

Results

Aldosterone increases $[Ca^{2+}]_i$ in preganglionic neurons of nucleus ambiguus

In rhodamine-labelled neurons, aldosterone (10^{-8} M) produced a fast and long-lasting increase in cytosolic Ca^{2+} concentration ($[Ca^{2+}]_i$; Fig. 1*A* and *B*); the increase in $[Ca^{2+}]_i$ reached a peak within 2 min after aldosterone treatment and maintained a long-lasting plateau (for about 10 min). G-36 (10^{-6} M), the GPER antagonist (Dennis *et al.* 2011), did not elicit a change in $[Ca^{2+}]_i$, but abolished the response to aldosterone (10^{-8} M; Fig. 1*A* and *B*); cells were treated with G-36

© 2013 The Authors. The Journal of Physiology © 2013 The Physiological Society

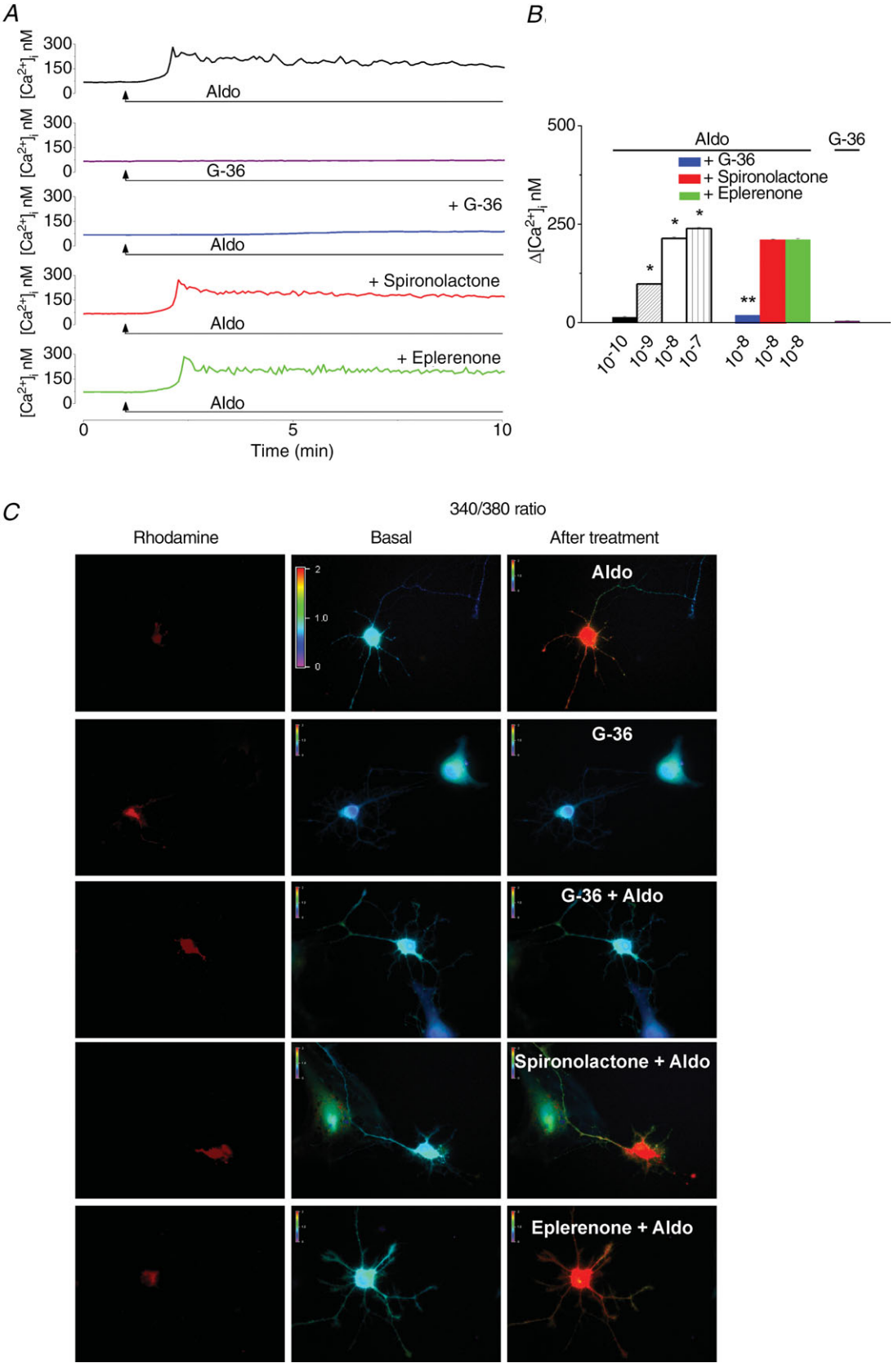

Figure 1. Aldosterone increases $[Ca^{2+}]_i$ in cardiac vagal preganglionic neurons of nucleus ambiguus via GPER activation

© 2013 The Authors. The Journal of Physiology © 2013 The Physiological Society

for 10 min before aldosterone and for the duration of aldosterone treatment. The mineralocorticoid receptor antagonists spironolactone (10^{-6} M) and eplerenone (10^{-6} M) did not significantly affect the Ca^{2+} response to aldosterone (Fig. 1*A*–*B*); the neurons were treated with spironolactone and eplerenone for 30 min before aldosterone and for the duration of aldosterone administration. Aldosterone (10^{-10}, 10^{-9}, 10^{-8} and 10^{-7} M) produced a dose-dependent increase in $[Ca^{2+}]_i$ by 14 ± 1.6 nM, 98 ± 1.7 nM, 214 ± 3.4 nM and 239 ± 3.1 nM, respectively ($n = 6$ for each concentration tested). Pre-treatment with the GPER antagonist G-36 (10^{-6} M, 10 min) abolished the response to aldosterone (10^{-8} M); $\Delta[Ca^{2+}]_i = 17 \pm 1.4$ nM in the presence of G-36 as compared to 214 ± 3.4 nM in the absence of the antagonist, while spironolactone or eplerenone did not significantly affect the aldosterone-induced Ca^{2+} response; $\Delta[Ca^{2+}]_i = 209 \pm 3.1$ nM in the presence of spironolactone, and 211 ± 2.8 nM in the presence of eplerenone (Fig. 1*B*). Representative examples of changes in 340/380 fluorescence ratio in rhodamine-labelled neurons of nucleus ambiguus in response to aldosterone in the absence and presence of the GPER and mineralocorticoid receptor antagonists are shown in Fig. 1*C*.

Aldosterone promotes Ca^{2+} release via inositol 1,4,5-trisphosphate (IP_3) and ryanodine receptors

In Ca^{2+}-free saline, aldosterone (10^{-8} M) produced a fast and transitory increase in $[Ca^{2+}]_i$ (Fig. 2*A*) with a lower amplitude than that occurring in Ca^{2+}-containing saline (Fig. 1*A* and *B*). The response elicited by aldosterone in Ca^{2+}-free saline was not significantly affected by blocking Ca^{2+} release from endo-lysosomes with Ned-19 (5 μM, 15 min; Naylor *et al.* 2009), while it was reduced by antagonism of ryanodine receptors with ryanodine (10 μM, 1 h), and abolished by blockade of IP_3 receptors with xestospongin C (XeC, 10 μM, 15 min) and 2-APB (100 μM, 15 min; Fig. 2*A*). Representative examples of aldosterone-induced Ca^{2+} responses are shown in Fig. 2*A* and the comparison of the amplitude of Ca^{2+} increases produced by aldosterone in Ca^{2+}-free saline, in the absence and presence of the antagonists, is shown in Fig. 2*B*. Aldosterone-induced increase in $[Ca^{2+}]_i$ in Ca^{2+}-free saline was 143 ± 2.9 nM; in the presence of Ned-19, $\Delta[Ca^{2+}]_i = 135 \pm 3.2$ nM ($n = 6$, $P > 0.05$); the response decreased to 81 ± 1.6 nM in the presence of ryanodine ($n = 6$, $P < 0.05$) and was practically abolished ($\Delta[Ca^{2+}]_i = 12 \pm 1.8$ nM) in the presence of xestospongin C and 2-APB (Fig. 2*B*).

Aldosterone promotes Ca^{2+} influx via voltage-gated P/Q channels

Since the Ca^{2+} response to aldosterone was reduced in Ca^{2+}-free saline, this indicates that Ca^{2+} influx, in addition to Ca^{2+} release from internal stores, is involved in aldosterone-induced increase in $[Ca^{2+}]_i$. We assessed the contribution of Ca^{2+} influx via voltage-gated L-, N- and P/Q-type Ca^{2+} channels in the Ca^{2+} response elicited by aldosterone. Blockade of L-type Ca^{2+} channels with nifedipine (1 μM, 10 min) or that of N-type channels with ω-conotoxin GVIA (100 nM, 10 min) did not significantly affect the response to aldosterone, while blockade of voltage-gated P/Q Ca^{2+} channels with ω-conotoxin MVIIC (100 nM, 10 min) markedly reduced the response; examples of representative recordings are shown in Fig. 3*A*. We assessed the amplitude of the increase in $[Ca^{2+}]_i$ produced by aldosterone at the peak and on the plateau phase of the response; comparison of the changes in amplitude in the presence of the Ca^{2+} channels blockers are shown in Fig. 3*B*. The mean amplitude of the aldosterone-induced increase in $[Ca^{2+}]_i$ in the absence of the blockers, on the plateau phase was 189 ± 2.8 nM; nifedipine and conotoxin GVIA did not significantly affect the Ca^{2+} response to aldosterone; on the plateau phase, $\Delta[Ca^{2+}]_i = 173 \pm 3.4$ nM, in the presence of nifedipine, and 186 ± 2.8 nM in the presence of conotoxin GVIA, as compared to 189 ± 2.8 nM in the absence of the blockers ($n = 6$ for each condition, $P > 0.05$), while conotoxin MVIIC (100 nM) abolished the plateau phase of the response to aldosterone ($\Delta[Ca^{2+}]_i = 6 \pm 1$ nM; $n = 6$, $P < 0.05$) and reduced the peak of the response (Fig. 3*B*).

Aldosterone depolarizes preganglionic vagal neurons of nucleus ambiguus

Aldosterone (10^{-8} M) produced a long-lasting depolarization of rhodamine-labelled neurons of nucleus

A, representative examples of Ca^{2+} responses upon administration of aldosterone (10^{-8} M) in the absence and presence of GPER antagonist G-36 and mineralocorticoid antagonists spironolactone and eplerenone. G-36 did not affect the $[Ca^{2+}]_i$, but abolished the response elicited by aldosterone. *B*, comparison of the Ca^{2+} responses elicited by increasing concentrations of aldosterone (Aldo, 10^{-10}, 10^{-9}, 10^{-8} and 10^{-7} M) in the presence of G-36 (10^{-6} M), spironolactone (10^{-6} M) and eplerenone (10^{-6} M); $^*P < 0.05$ as compared to basal $[Ca^{2+}]_i$ levels; $^{**}P < 0.05$ as compared with Ca^{2+} response induced by aldosterone (10^{-8} M). *C*, Fura-2 AM fluorescence ratio (340 nm/380 nm) of rhodamine-labelled neurons, before and after treatment with aldosterone (Aldo, 10^{-8} M) in the absence and presence of G-36, spironolactone and eplerenone; hot colours indicate an increased fluorescence ratio, cold colours indicate low fluorescence ratio.

© 2013 The Authors. The Journal of Physiology © 2013 The Physiological Society

ambiguus (Fig. 4*A*). The GPER antagonist G-36 (10^{-6} M), while not producing any change in membrane potential, when applied alone abolished the depolarization induced by aldosterone (10^{-8} M; Fig. 4*A*). On the other hand, aldosterone-induced depolarization was not affected by spironolactone (10^{-6} M) or eplerenone (10^{-6} M); the neurons were treated with the mineralocorticoid antagonists for 30 min before aldosterone and for the duration of aldosterone application (Fig. 4*A*). The mean amplitude of depolarization produced by aldosterone (10^{-10}, 10^{-9}, 10^{-8} and 10^{-7} M) was 0.27 ± 0.16 mV, 1.19 ± 0.37 mV, 5.8 ± 0.81 mV and 6.34 ± 0.63 mV,

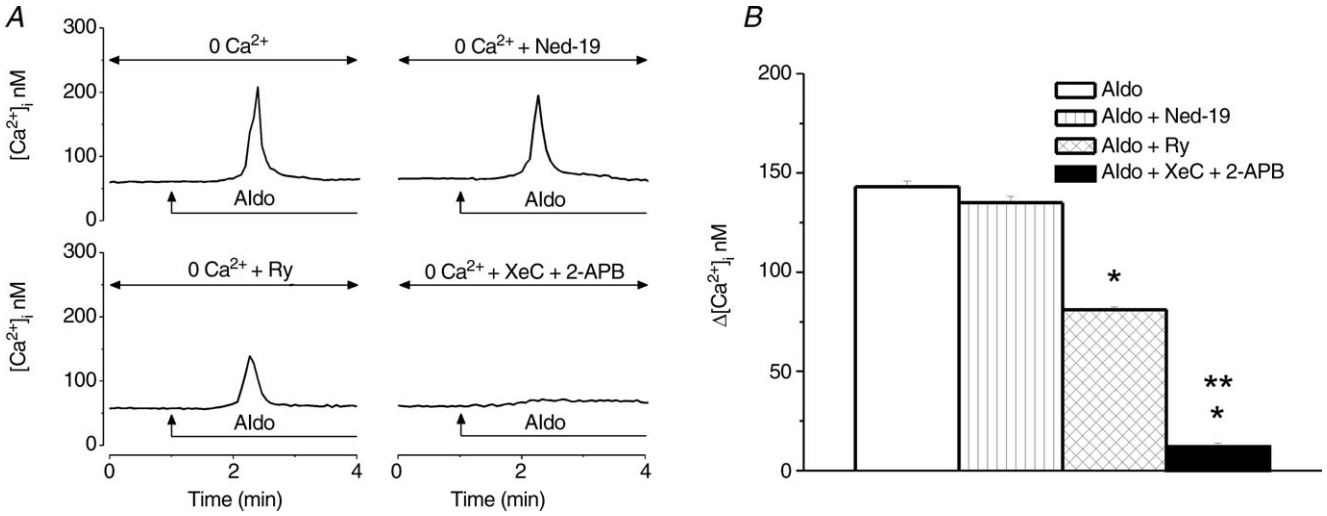

Figure 2. Aldosterone promotes Ca^{2+} release via IP_3 and ryanodine receptors
A, representative examples of increases in $[Ca^{2+}]_i$ produced by aldosterone (10^{-8} M) in Ca^{2+}-free saline before (top left) or after treatment with Ned-19 (1 μM, top right), ryanodine (Ry, 10 μM, bottom left) or xestospongin C (XeC, 10 μM) and 2-APB (100 μM, bottom right); the arrows indicate the treatment with aldosterone. *B*, comparisons of mean amplitude ± SEM of $[Ca^{2+}]_i$ increases produced by aldosterone in Ca^{2+}-free saline and the blocker(s) mentioned (*$P < 0.05$ compared to the response to aldosterone alone; **$P < 0.05$ as compared to $[Ca^{2+}]_i$ increases produced by aldosterone in the presence of ryanodine).

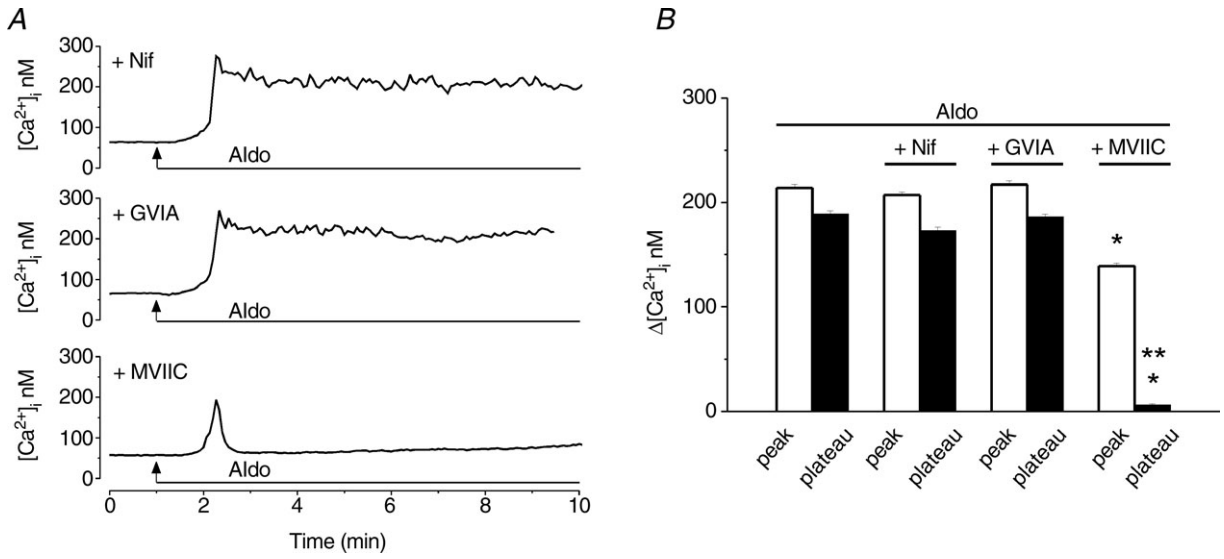

Figure 3. Aldosterone promotes Ca^{2+} influx through P/Q-type voltage-gated Ca^{2+} channels
A, representative traces illustrating the Ca^{2+} responses of nucleus ambiguus neurons to aldosterone (10^{-8} M) treatment in the presence of nifedipine (L-type Ca^{2+} channel blocker, 1 μM, top), ω-conotoxin GVIA (GVIA, N-type Ca^{2+} channel blocker, 100 nM, middle) or ω-conotoxin MVIIC (MVIIC, P/Q-type Ca^{2+} channel blocker, 100 nM, bottom). *B*, comparison of the mean amplitude ± SEM of $[Ca^{2+}]_i$ increases produced by aldosterone at the peak and on the plateau of the response in the indicated conditions; $P < 0.05$ as compared to the peak (*) or plateau (**) of the Ca^{2+} response produced by aldosterone alone.

© 2013 The Authors. The Journal of Physiology © 2013 The Physiological Society

respectively ($n = 6$ for each concentration). Pretreatment with G-36 (10^{-6} M, 10 min) abolished the response to aldosterone (Δvoltage $= -0.43 \pm 0.09$ mV), while pretreatment with spironolactone (10^{-6} M) or eplerenone (10^{-6} M) did not significantly affect the depolarization induced by aldosterone (Δvoltage $= 5.7 \pm 0.72$ mV and 5.5 ± 0.84 mV in the presence of spironolactone and eplerenone, respectively, as compared to 5.8 ± 0.81 mV in the absence of the antagonists; $n = 6$, $P > 0.05$; Fig. 4*B*).

Functional identification of nucleus ambiguus

Microinjection of control saline into nucleus ambiguus did not affect the heart rate, while microinjection of L-glutamate (L-Glu, 5×10^{-3} M, 50 nl) at the same site elicited a bradycardic response in anaesthetized rats (Fig. 5*A*), as previously reported (Chitravanshi *et al.* 2009, 2012; Brailoiu *et al.* 2013), indicating the correct placement of the cannula. The bradycardic effect induced by microinjection of L-glutamate was prevented by I.V. injection of atropine (2 mg kg^{-1}), a potent muscarinic receptor antagonist (Fig. 5*A*), indicating that the response was cholinergic-mediated. The comparison of the amplitude of the heart rate change produced by control saline, L-glutamate, and L-glutamate after atropine, is illustrated in Fig. 5*B*. In anaesthetized rats, microinjection of L-glutamate into the nucleus ambiguus decreased the heart rate by 76 ± 2.5 beats min^{-1} ($n = 5$).

Microinjection of aldosterone into nucleus ambiguus decreases the heart rate in awake rats

In conscious, freely moving rats bearing a cannula implanted into nucleus ambiguus, microinjection of control saline did not modify the heart rate, while microinjection of L-glutamate (L-Glu, 5×10^{-3} M, 50 nl) elicited a bradycardic response (Fig. 6*A*) similar to that previously reported in anaesthetized rats (Chitravanshi *et al.* 2009, 2012; Brailoiu *et al.* 2013). Microinjection of aldosterone (10^{-7} M, 50 nl), or G-1 (10^{-5} M), the synthetic GPER agonist (Bologa *et al.* 2006), or concomitant microinjection of aldosterone and G-1, at the same site, produced a decrease in heart rate; representative examples are shown in Fig. 6*A*. A comparison of the amplitude of the heart rate changes produced by microinjection of the compounds is shown in Fig. 6*B*. In conscious rats, microinjection of L-glutamate (5×10^{-3} M, 50 nl) into the nucleus ambiguus reduced the heart rate by 89 ± 3.5 beats min^{-1} ($n = 5$). Microinjection of aldosterone (10^{-10} M, 10^{-9} M, 10^{-8} M, 10^{-7} M and 10^{-6} M; 50 nl) produced a dose-dependent decrease in heart rate by 6 ± 2, 18 ± 1.7, 31 ± 2.9, 46 ± 2.8 and 45 ± 3.1 beats min^{-1}, respectively ($n = 5$). Microinjection of G-1 (10^{-5} M) that produced a maximal bradycardic response in our previous study in anaesthetized rats (Brailoiu *et al.* 2013) elicited a decrease in heart rate by 64 ± 3.1 beats min^{-1} (Fig. 6*B*). Concomitant microinjection of G-1 (10^{-5} M) and aldosterone (10^{-7} M),

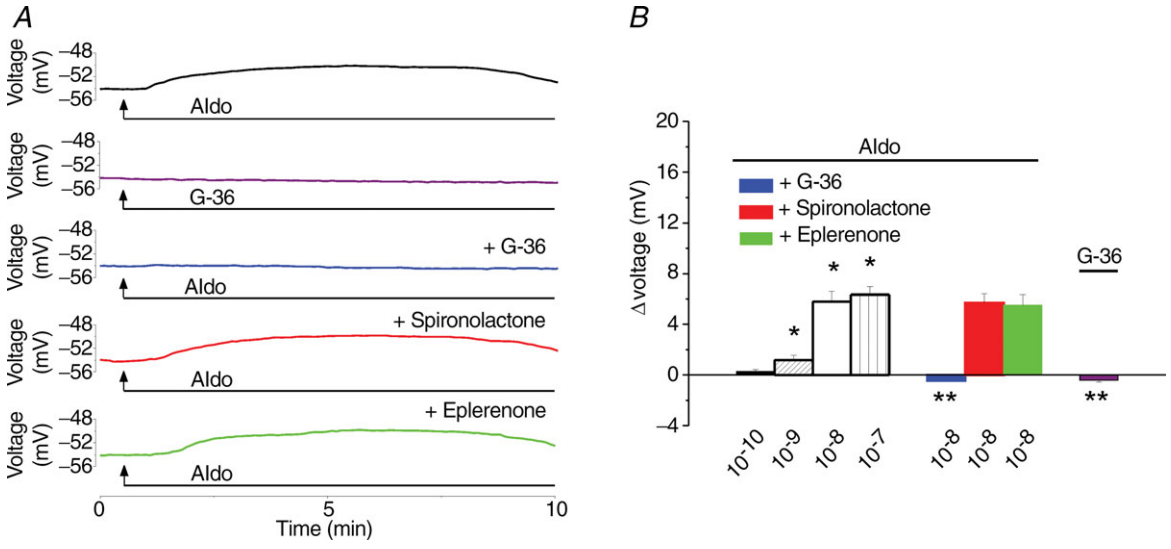

Figure 4. Aldosterone elicits depolarization of cardiac preganglionic neurons of nucleus ambiguus
A, representative recordings illustrating changes in membrane potential of cardiac vagal neurons upon application of aldosterone (10^{-8} M), G-36 (10^{-6} M) alone, and aldosterone (10^{-8} M), in the presence of the GPER antagonist G-36 (10^{-6} M) or of the mineralocorticoid receptor antagonists spironolactone (10^{-6} M) and eplerenone (10^{-6} M). *B*, aldosterone (10^{-10}, 10^{-9}, 10^{-8} and 10^{-7} M) produces a concentration-dependent depolarization of nucleus ambiguus neurons. The response to 10^{-8} M aldosterone is sensitive to antagonism of GPER by G-36, but not to the antagonism of mineralocorticoid receptor by spironolactone or eplerenone; $P < 0.05$ compared to basal membrane potential (*) or to the depolarization induced by 10^{-8} M aldosterone (**).

© 2013 The Authors. The Journal of Physiology © 2013 The Physiological Society

decreased heart rate by 63 ± 3.4 beats min^{-1} (Fig. 6*B*), that was not significantly different from G-1 alone ($P > 0.05$).

Aldosterone-induced bradycardia is blocked by the GPER antagonist in awake rats

In the next series of experiments we tested the sensitivity of the bradycardic response elicited by aldosterone to the antagonism of GPER and mineralocorticoid receptors. Microinjection of G-36 (10^{-6} M), the GPER antagonist, into the nucleus ambiguus, did not produce a significant change in heart rate; concomitant microinjection of G-36 (10^{-6} M) and aldosterone (10^{-8} M), abolished the bradycardia elicited by aldosterone (Fig. 7*A*). Microinjection of spironolactone (10^{-6} M) or eplerenone (10^{-6} M) concomitant with aldosterone (10^{-8} M), did not produce a noticeable effect on aldosterone-induced bradycardia (Fig. 7*A*). Comparison of the changes in heart rate elicited by the microinjection into nucleus ambiguus of aldosterone in the absence and presence of the GPER and mineralocorticoid antagonists is illustrated in Fig. 7*B*. The bradycardic response elicited by aldosterone (10^{-8} M) was abolished by G-36 (10^{-6} M); in the presence of G-36, aldosterone increased the heart rate by 11 ± 1.8 beats min^{-1}. Microinjection of G-36 (10^{-6} M) alone produced an insignificant increase in heart rate by 10 ± 1.9 beats min^{-1} ($P > 0.05$). Spironolactone

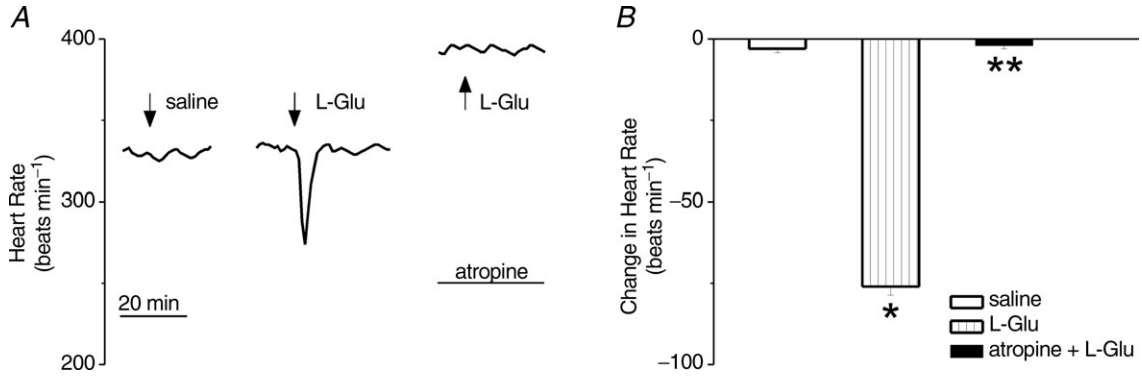

Figure 5. Control microinjections and functional identification of nucleus ambiguus
A, examples of changes in heart rate after microinjection of control saline, L-glutamate (L-Glu, 5 × 10^{-3} M, 50 nl) and L-Glu after atropine (2 mg kg^{-1}) in anaesthetized rats; L-Glu-induced bradycardia was abolished by atropine. *B*, comparison of the heart rate changes produced by microinjection of saline, L-Glu and L-Glu after atropine; *$P < 0.05$ and **$P > 0.05$ as compared to control saline injection.

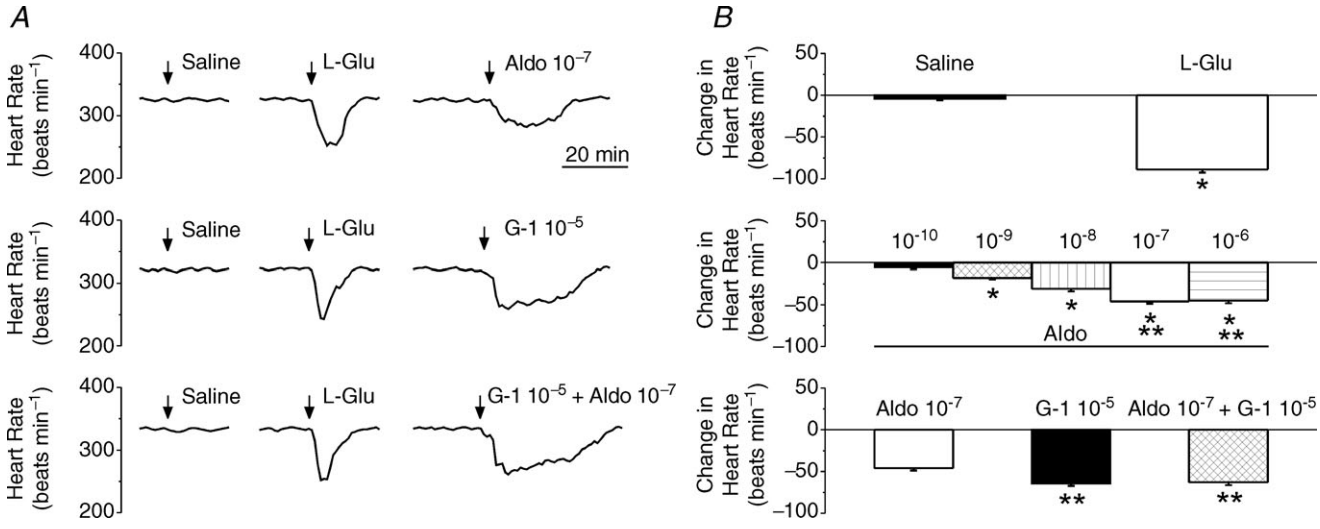

Figure 6. Microinjection of aldosterone into nucleus ambiguus elicits bradycardia in conscious rats
A, example of changes in heart rate after microinjection of control saline, L-glutamate (L-Glu, 5 × 10^{-3} M, 50 nl), aldosterone (Aldo, 10^{-7} M, 50 nl), G-1 (10^{-5} M, 50 nl) and concomitant microinjection of aldosterone (10^{-7} M) and G-1 (10^{-5} M). *B*, comparison of the heart rate changes produced by microinjection in the nucleus ambiguus of saline, L-Glu, aldosterone and G-1, in conscious rats. Aldosterone (10^{-10} to 10^{-6} M) produced a dose-dependent decrease in heart rate. Comparison of the amplitude of bradycardia produced by maximal doses of aldosterone (10^{-7} M) and G-1(10^{-5} M). *$P < 0.05$; **$P > 0.05$.

© 2013 The Authors. The Journal of Physiology © 2013 The Physiological Society

(10^{-6} M) or eplerenone (10^{-6} M) did not significantly affect the bradycardic response induced by aldosterone; the heart rate decreased by 29 ± 1.6 beats min^{-1} in the presence of aldosterone and spironolactone and by 32 ± 2.4 beats min^{-1} in the presence of aldosterone and eplerenone as compared to a decrease by 31 ± 2.9 beats min^{-1} produced by the same dose (10^{-8} M) of aldosterone alone ($n = 5$; Fig. 7*B*).

Discussion

Increasing evidence supports the non-genomic actions of aldosterone (for review see Funder, 2005). Despite the fact that the receptors mediating faster effects of aldosterone remained unclear, recent evidence indicates that GPER mediates non-genomic effects of aldosterone (Gros *et al.* 2011*a*,*b*, 2013; Feldman & Gros, 2011; Funder, 2011). We have previously reported that GPER is expressed in nucleus ambiguus neurons (Brailoiu *et al.* 2007) and its activation leads to bradycardia (Brailoiu *et al.* 2013). In the current study we examined the effect of aldosterone on cardiac vagal neurons of nucleus ambiguus using *in vitro* and *in vivo* approaches.

Since one of the non-genomic effects associated with aldosterone action is an increase in cytosolic Ca^{2+} concentration ($[Ca^{2+}]_i$; Wehling *et al.* 1995; Schneider *et al.* 1997; Estrada *et al.* 2000; Harvey & Higgins, 2000), and GPER activation increases cytosolic Ca^{2+} in several cellular models (Revankar *et al.* 2005; Brailoiu *et al.* 2007; Tica *et al.* 2011: Deliu *et al.* 2012; Brailoiu *et al.* 2013) we first used calcium imaging to examine the effects of aldosterone in cardiac-projecting neurons of nucleus ambiguus. Neurons were retrogradely labelled with rhodamine, a reliable marker for identification of cardiac preganglionic vagal neurons (Bouairi *et al.* 2006; Brailoiu *et al.* 2012, 2013).

Aldosterone increased cytosolic Ca^{2+} concentration in rhodamine-labelled cardiac vagal neurons of nucleus ambiguus in a dose-dependent manner. Similarly, aldosterone has been reported to increase cytosolic Ca^{2+} in other cell models such as human colon cells (Doolan *et al.* 1998), rat vascular smooth muscle cells (Wehling *et al*. 1995), and porcine endothelial cells (Schneider *et al.* 1997). In addition, in nucleus ambiguus neurons, the Ca^{2+} response elicited by aldosterone was prevented by G-36, an antagonist of GPER, supporting the involvement of GPER. We have recently reported that another GPER synthetic agonist, G-1 (Bologa *et al.* 2006) increased cytosolic Ca^{2+} in cardiac vagal neurons of nucleus ambiguus; similarly, the effect of G-1 on Ca^{2+} was abolished by G-36 (Brailoiu *et al.* 2013). With respect to the increase in cytosolic Ca^{2+} produced, aldosterone was more potent, but less efficacious than G-1. The increase in cytosolic Ca^{2+} produced by aldosterone was faster, reaching a peak within 2 min after aldosterone treatment, and maintained a long-lasting plateau (for about 10 min).

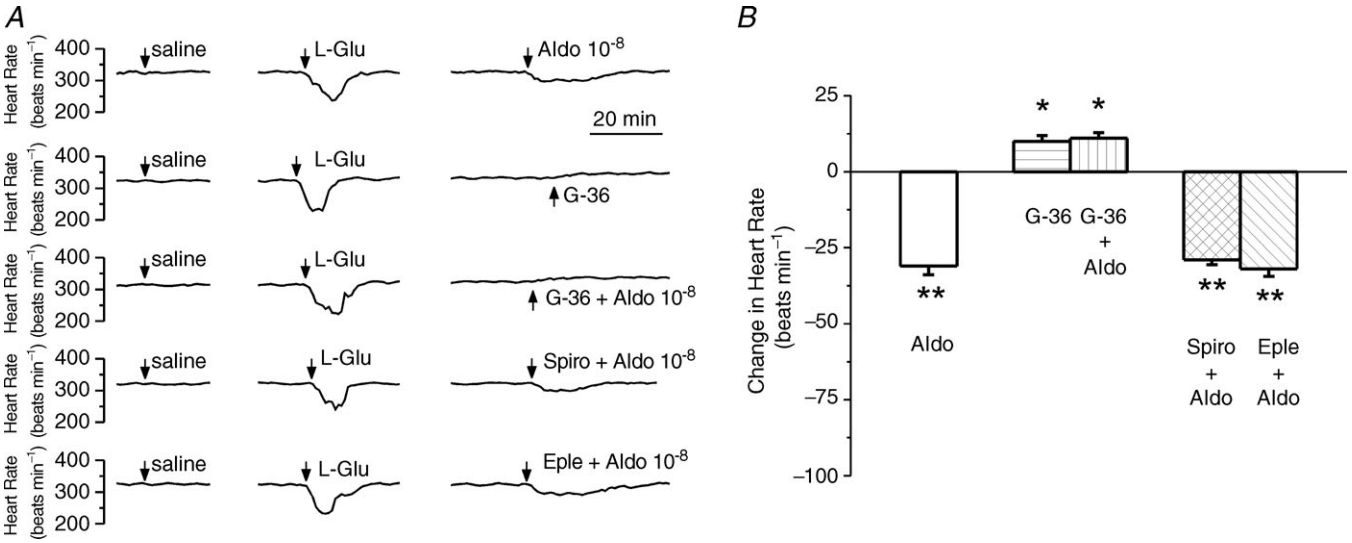

Figure 7. Aldosterone-induced bradycardia is mediated by GPER
A, example of changes in heart rate after microinjection of control saline, L-glutamate (L-Glu, 5×10^{-3} M, 50 nl), aldosterone (Aldo, 10^{-8} M, 50 nl), G-36 (10^{-6} M) and aldosterone (Aldo, 10^{-8} M, 50 nl) in the presence of G-36 (10^{-6} M), spironolactone (10^{-6} M) or eplerenone (10^{-6} M). The decrease in heart rate produced by aldosterone (10^{-8} M) was abolished by the GPER antagonist, G-36 (10^{-6} M), while not affected by the mineralocorticoid receptor antagonists spironolactone (10^{-6} M) and eplerenone (10^{-6} M). *B*, comparison of the change in heart rate induced by microinjection into nucleus ambiguus of aldosterone in the absence and presence of GPER and mineralocorticoid receptor antagonists. $^*P < 0.05$ and $^{**}P > 0.05$ as compared to bradycardia induced by 10^{-8} M aldosterone.

© 2013 The Authors. The Journal of Physiology © 2013 The Physiological Society

Similarly, aldosterone produced a fast-onset increase in cytosolic Ca^{2+} followed by a plateau, in skin cells from mineralocorticoid receptor knockout mice (Haseroth *et al.* 1999). On the other hand, in nucleus ambiguus neurons, the increase in cytosolic Ca^{2+} occurred 5–6 min after G-1 administration and was also followed by a sustained increase (Brailoiu *et al.* 2013). The delayed response to G-1 was similar to our previous findings in hypothalamus neurons (Brailoiu *et al*. 2007), spinal cord neurons (Deliu *et al*. 2012), or in myometrial cells (Tica *et al.* 2011). These differences in the Ca^{2+} response elicited by G-1 and aldosterone may be due to differences in drug–receptor interaction for GPER agonists. While the activation of GPER by oestrogen, an endogenous agonist, and G-1, a synthetic agonist, has been extensively studied (Revankar *et al.* 2005; Bologa *et al.* 2006; Prossnitz & Barton, 2011), there is limited information on the pharmacology of aldosterone–GPER interaction.

Another notable observation was that aldosterone-induced increase in cytosolic Ca^{2+} was not affected by administration of mineralocorticoid antagonists spironolactone and eplerenone, in concentrations that reduced the response to aldosterone in other cellular models (Gros *et al.* 2011*b*). The aldosterone-induced Ca^{2+} response in skeletal muscle cells was also insensitive to spironolactone (Estrada *et al*. 2000).

With respect to the source of Ca^{2+}, we found that both Ca^{2+} release from internal stores and Ca^{2+} influx were involved. In human colon cells (Doolan *et al.* 1998), vascular smooth muscle cells (Wehling *et al.* 1995), and porcine endothelial cells (Schneider *et al.* 1997), the predominant mechanism of aldosterone-induced Ca^{2+} increase was Ca^{2+} release from internal stores. In nucleus ambiguus neurons, aldosterone releases Ca^{2+} via activation of IP_3 receptors, and less via ryanodine receptors. IP_3 receptors and ryanodine receptors are Ca^{2+}-release channels located predominantly on the endoplasmic reticulum (Berridge, 1998). The endoplasmic reticulum Ca^{2+} store is sensitive to thapsigargin, an inhibitor of the sarcoplasmic/endoplasmic reticulum ATPase. Similarly, in rat and rabbit aortic smooth muscle cells, aldosterone mobilizes Ca^{2+} from endoplasmic reticulum thapsigargin-sensitive stores (Wehling *et al.* 1995). On the other hand, endo-lysosomal Ca^{2+} stores did not seem to play a role in Ca^{2+} mobilization by aldosterone in nucleus ambiguus, as blocking of Ca^{2+} release from endo-lysosomes with Ned-19 (Naylor *et al.* 2009) failed to affect the Ca^{2+} response elicited by aldosterone.

In addition to Ca^{2+} release from endoplasmic reticulum, aldosterone induced Ca^{2+} influx via P/Q-type Ca^{2+} channels, but not via L-type and N-type Ca^{2+} channels in nucleus ambiguus neurons. P/Q channels are the predominant type of voltage-gated Ca^{2+} channels identified in these neurons (Irnaten *et al.* 2003). Similar to aldosterone, urocortin 3 also activates P/Q Ca^{2+} channels in nucleus ambiguus neurons (Chitravanshi *et al.* 2012, Brailoiu *et al*. 2012).

Further, aldosterone induced a depolarization of nucleus ambiguus neurons that was sensitive to antagonism of GPER but not of mineralocorticoid receptors. The depolarization had a similar time course to the Ca^{2+} increase elicited by aldosterone; it is possible that the depolarization induced by aldosterone triggered the Ca^{2+} influx by P/Q channels. The Ca^{2+} influx may further increase Ca^{2+} signals by activating ryanodine receptors via a Ca^{2+}-induced Ca^{2+} release mechanism. Similar to the Ca^{2+} signal elicited by aldosterone, with respect to the depolarization induced, aldosterone was more potent but less efficacious than G-1. The depolarization induced by aldosterone also had a faster onset: it started around 1 min after the administration of aldosterone and it was long-lasting, while the depolarization to G-1 was slower, reaching the peak within 5 min (Brailoiu *et al.* 2013), suggesting an agonist-selective interaction with the receptor.

We tested the significance of our *in vitro* findings by *in vivo* telemetric measurement of the heart rate in response to microinjection of aldosterone into the nucleus ambiguus. To prevent any potential interference of anaesthetics with the cardiovascular reflexes (Irnaten *et al.* 2002*a*,*b*) as well as handling of the rats, which may act as a stressor (McDougall *et al*. 2004), we examined the effect of aldosterone in conscious, freely moving rats. Microinjection of aldosterone into the nucleus ambiguus induces bradycardia, as previously reported by the synthetic GPER agonist, G-1, in anaesthetized rats (Brailoiu *et al.* 2013). Aldosterone-induced bradycardia was dose-dependent and not affected by the mineralocorticoid antagonists spironolactone and eplerenone, unlike previous findings in vascular smooth muscle and endothelial cells, where both GPER and mineralocorticoid receptors contributed to the effects of aldosterone (Gros *et al.* 2011*a*,*b*). Aldosterone-induced bradycardia was abolished by the GPER antagonist G-36. Similarly, a recent study indicates that the vascular effects of aldosterone or G-1 were blocked by another GPER antagonist, G-15 (Gros *et al*. 2013).

To further verify whether or not GPER is a common effector for G-1 and aldosterone, we tested the effect of concomitant microinjection of maximal doses of G-1 and aldosterone into the nucleus ambiguus; the two agonists did not produce a higher bradycardic response, as compared to G-1 alone, supporting GPER as a common pathway for the effects of G-1 and aldosterone.

Our results indicate that the activation of nucleus ambiguus neurons by aldosterone is mediated by GPER without an involvement of mineralcorticoid receptors, as previously reported in other cellular models (Gros *et al.* 2011*a*,*b*). In addition, our results do not support a role for eplerenone as a GPER antagonist, as previously suggested (Funder, 2011). Lower concentrations

© 2013 The Authors. The Journal of Physiology © 2013 The Physiological Society

of aldosterone tested in our study mimic those present in physiological settings (Schirpenbach *et al.* 2006), while higher concentrations are associated with hypertension, hyperaldosteronism and heart failure (Weber, 2001; Losel *et al.* 2004). Moreover, aldosterone synthesis occurs in the brain and has been involved in cardiovascular regulation (Gomez-Sanchez *et al.* 2010). For example, the aldosterone concentration in the rat hypothalamus is around 350 pg g^{-1} (Huang *et al.* 2009).

The physiological and pathophysiological significance of the increase in cardiac vagal tone by aldosterone remains to be determined; it may be part of a compensatory mechanism. Our results also propose a new mechanism for an earlier reported increase in the cardiac vagal tone by aldosterone in healthy humans (Heindl *et al.* 2006). Moreover, the current findings indicate that GPER, in addition to mediating the effects of aldosterone on cell growth and vascular reactivity (Gros *et al.* 2011*a*,*b*, 2013), also mediates neuronal effects of aldosterone.

References

Benamar K, Addou S, Yondorf M, Geller EB, Eisenstein TK & Adler MW (2010). Intrahypothalamic injection of the HIV-1 envelope glycoprotein induces fever via interaction with the chemokine system. *J Pharmacol Exp Ther* **332**, 549–553.

Berridge MJ (1998). Neuronal calcium signalling. *Neuron* **21**, 13–26.

Bologa CG, Revankar CM, Young SM, Edwards BS, Arterburn JB, Kiselyov AS, Parker MA, Tkachenko SE, Savchuck NP, Sklar LA, Oprea TI & Prossnitz ER (2006). Virtual and biomolecular screening converge on a selective agonist for GPR30. *Nat Chem Biol* **2**, 207–212.

Bouairi E, Kamendi H, Wang X, Gorini C & Mendelowitz D (2006). Multiple types of $GABA_A$ receptors mediate inhibition in brain stem parasympathetic cardiac neurons in the nucleus ambiguus. *J Neurophysiol* **96**, 3266–3272.

Brailoiu E, Dun SL, Brailoiu GC, Mizuo K, Sklar LA, Oprea TI, Prossnitz ER & Dun NJ (2007). Distribution and characterization of estrogen receptor G protein-coupled receptor 30 in the rat central nervous system. *J Endocrinol* **193**, 311–321.

Brailoiu GC, Arterburn JB, Oprea TI, Chitravanshi VC & Brailoiu E (2013). Bradycardic effects mediated by activation of G protein-coupled estrogen receptor in rat nucleus ambiguus. *Exp Physiol* **98**, 679–691.

Brailoiu GC, Deliu E, Tica AA, Chitravanshi VC & Brailoiu E (2012). Urocortin 3 elevates cytosolic calcium in nucleus ambiguus neurons. *J Neurochem* **122**, 1129–1136.

Brailoiu GC, Gurzu B, Gao X, Parkesh R, Aley PK, Trifa DI, Galione A, Dun NJ, Madesh M, Patel S, Churchill GC & Brailoiu E (2010). Acidic NAADP-sensitive calcium stores in the endothelium: agonist-specific recruitment and role in regulating blood pressure. *J Biol Chem* **285**, 37133–37137.

Brauner T, Hulser DF & Strasser RJ (1984). Comparative measurements of membrane potentials with microelectrodes and voltage-sensitive dyes. *Biochim Biophys Acta* **771**, 208–216.

Chitravanshi VC, Bhatt S & Sapru HN (2009). Microinjections of α-melanocyte stimulating hormone into the nucleus ambiguus of the rat elicit vagally mediated bradycardia. *Am J Physiol Regul Integr Comp Physiol* **296**, R1402–R1411.

Chitravanshi VC, Kawabe K & Sapru HN (2012). Bradycardic effects of microinjections of urocortin 3 into the nucleus ambiguus of the rat. *Am J Physiol Regul Integr Comp Physiol* **303**, R1023–1030.

Deliu E, Brailoiu GC, Arterburn JB, Oprea TI, Benamar K, Dun NJ & Brailoiu E (2012). Mechanisms of G protein-coupled estrogen receptor-mediated spinal nociception. *J Pain* **13**, 742–754.

Dennis MK, Field AS, Burai R, Ramesh C, Petrie WK, Bologa CG, Oprea TI, Yamaguchi Y, Hayashi S, Sklar LA, Hathaway HJ, Arterburn JB & Prossnitz ER (2011). Identification of a GPER/GPR30 antagonist with improved estrogen receptor counterselectivity. *J Steroid Biochem Mol Biol* **127**, 358–366.

Doolan CM, O'Sullivan GC & Harvey BJ (1998). Rapid effects of corticosteroids on cytosolic protein kinase C and intracellular calcium concentration in human distal colon. *Mol Cell Endocrinol* **138**, 71–79.

Estrada M, Liberona JL, Miranda M & Jaimovich E (2000). Aldosterone- and testosterone-mediated intracellular calcium response in skeletal muscle cell cultures. *Am J Physiol Endocrinol Metab* **279**, E132–E139.

Feldman RD & Gros R (2011). Unraveling the mechanisms underlying the rapid vascular effects of steroids: sorting out the receptors and the pathways. *Br J Pharmacol* **163**, 1163–1169.

Funder JW (2005). The nongenomic actions of aldosterone. *Endocr Rev* **26**, 313–321.

Funder JW (2011). GPR30, mineralocorticoid receptors, and the rapid vascular effects of aldosterone. *Hypertension* **57**, 370–372.

Gomez-Sanchez EP, Gomez-Sanchez CM, Plonczynski M & Gomez-Sanchez CE (2010). Aldosterone synthesis in the brain contributes to Dahl salt-sensitive rat hypertension. *Exp Physiol* **95**, 120–130.

Gros R, Ding Q, Davis M, Shaikh R, Liu B, Chorazyczewski J, Pickering JG & Feldman RD (2011*a*). Delineating the receptor mechanisms underlying the rapid vascular contractile effects of aldosterone and estradiol. *Can J Physiol Pharmacol* **89**, 655–663.

Gros R, Ding Q, Liu B, Chorazyczewski J & Feldman RD (2013). Aldosterone mediates its rapid effects in vascular endothelial cells through GPER activation. *Am J Physiol Cell Physiol* **304**, C532–C540.

Gros R, Ding Q, Sklar LA, Prossnitz EE, Arterburn JB, Chorazyczewski J & Feldman RD (2011*b*). GPR30 expression is required for the mineralocorticoid receptor-independent rapid vascular effects of aldosterone. *Hypertension* **57**, 442–451.

Grynkiewicz G, Poenie M & Tsien RY (1985). A new generation of Ca^{2+} indicators with greatly improved fluorescence properties. *J Biol Chem* **260**, 3440–3450.

© 2013 The Authors. The Journal of Physiology © 2013 The Physiological Society

Harvey BJ & Higgins M (2000). Nongenomic effects of aldosterone on Ca^{2+} in M-1 cortical collecting duct cells. *Kidney Int* **57**, 1395–1403.

Haseroth K, Gerdes D, Berger S, Feuring M, Gunther A, Herbst C, Christ M & Wehling M (1999). Rapid nongenomic effects of aldosterone in mineralocorticoid-receptor-knockout mice. *Biochem Biophys Res Commun* **266**, 257–261.

Heindl S, Holzschneider J, Hinz A, Sayk F, Fehm HL & Dodt C (2006). Acute effects of aldosterone on the autonomic nervous system and the baroreflex function in healthy humans. *J Neuroendocrinol* **18**, 115–121.

Huang BS, White RA, Jeng AY & Leenen FH (2009). Role of central nervous system aldosterone synthase and mineralocorticoid receptors in salt-induced hypertension in Dahl salt-sensitive rats. *Am J Physiol Regul Integr Comp Physiol* **296**, R994–R1000.

Irnaten M, Aicher SA, Wang J, Venkatesan P, Evans C, Baxi S & Mendelowitz D (2003). μ-Opioid receptors are located postsynaptically and endomorphin-1 inhibits voltage-gated calcium currents in premotor cardiac parasympathetic neurons in the rat nucleus ambiguus. *Neuroscience* **116**, 573–582.

Irnaten M, Wang J, Chang KS, Andresen MC & Mendelowitz D (2002*a*). Ketamine inhibits sodium currents in identified cardiac parasympathetic neurons in nucleus ambiguus. *Anesthesiology* **96**, 659–666.

Irnaten M, Wang J, Venkatesan P, Evans CBA, Chang KS, Andresen MC & Mendelowitz D (2002*b*). Ketamine inhibits presynaptic and postsynaptic nicotinic excitation of identified cardiac parasympathetic neurons in nucleus ambiguus. *Anesthesiology* **96**, 667–674.

Liu SL, Schmuck S, Chorazcyzewski JZ, Gros R & Feldman RD (2003). Aldosterone regulates vascular reactivity: short-term effects mediated by phosphatidylinositol 3-kinase-dependent nitric oxide synthase activation. *Circulation* **108**, 2400–2406.

Losel R, Schultz A, Boldyreff B & Wehling M (2004). Rapid effects of aldosterone on vascular cells: clinical implications. *Steroids* **69**, 575–578.

McDougall SJ, Lawrence AJ & Widdop RE (2005). Differential cardiovascular responses to stressors in hypertensive and normotensive rats. *Exp Physiol* **90**, 141–150.

Naylor E, Arredouani A, Vasudevan SR, Lewis AM, Parkesh R, Mizote A, Rosen D, Thomas JM, Izumi M, Ganesan A, Galione A & Churchill GC (2009). Identification of a chemical probe for NAADP by virtual screening. *Nat Chem Biol* **5**, 220–226.

Paxinos G & Watson C (1998). The Rat Brain in Stereotaxic Coordinates. Fourth Edition. Academic Press, San Diego.

Prossnitz ER & Barton M. The G-protein-coupled estrogen receptor GPER in health and disease (2011). *Nat Rev Endocrinol* **16**, 715–726.

Revankar CM, Cimino DF, Sklar LA, Arterburn JB & Prossnitz ER (2005). A transmembrane intracellular estrogen receptor mediates rapid cell signalling. *Science* **307**, 1625–1630.

Schirpenbach C, Seiler L, Maser-Gluth C, Beuschlein F, Reincke M & Bidlingmaier M (2006). Automated chemiluminescence-immunoassay for aldosterone during dynamic testing: comparison to radioimmunoassays with and without extraction steps. *Clin Chem* **52**, 1749–1755.

Schmidt BM, Horisberger K, Feuring M, Schultz A & Wehling M (2005). Aldosterone blunts human baroreflex sensitivity by a nongenomic mechanism. *Exp Clin Endocrinol Diabetes* **113**, 252–256.

Schmidt BM, Montealegre A, Janson CP, Martin N, Stein-Kemmesies C, Scherhag A, Feuring M, Christ M & Wehling M (1999). Short term cardiovascular effects of aldosterone in healthy male volunteers. *J Clin Endocrinol Metab* **84**, 3528–3533.

Schmidt BM, Oehmer S, Delles C, Bratke R, Schneider MP, Klingbeil A, Fleischmann EH & Schmieder RE (2003). Rapid nongenomic effects of aldosterone on human forearm vasculature. *Hypertension* **42**, 156–160.

Schneider M, Ulsenheimer A, Christ M & Wehling M (1997). Nongenomic effects of aldosterone on intracellular calcium in porcine endothelial cells. *Am J Physiol Endocrinol Metab* **272**, E616–E620.

Schöniger S, Wehming S, Gonzalez C, Schöbitz K, Rodríguez E, Oksche A, Yulis CR & Nürnberger F (2001). The dispersed cell culture as model for functional studies of the subcommissural organ: preparation and characterization of the culture system. *J Neurosci Methods* **107**, 47–61.

Tica AA, Dun EC, Tica OS, Gao X, Arterburn JB, Brailoiu GC, Oprea TI & Brailoiu E (2011). G protein-coupled estrogen receptor 1-mediated effects in the rat myometrium. *Am J Physiol Cell Physiol* **301**, C1262–C1269.

Weber KT (2001). Aldosterone in congestive heart failure. *N Engl J Med* **345**, 1689–1697.

Wehling M (1997). Specific, nongenomic actions of steroid hormones. *Annu Rev Physiol* **59**, 365–393.

Wehling M, Neylon CB, Fullerton M, Bobik A & Funder JW (1995). Nongenomic effects of aldosterone on intracellular Ca^{2+} in vascular smooth muscle cells. *Circ Res* **76**, 973–979.

Wehling M, Spes CH, Win N, Janson CP, Schmidt BM, Theisen K & Christ M (1998). Rapid cardiovascular action of aldosterone in man. *J Clin Endocrinol Metab* **83**, 3517–3522.

Yee KM & Struthers AD (1998). Aldosterone blunts the baroreflex response in man. *Clin Sci (Lond)* **95**, 687–692.

Yu Y, Wei SG, Zhang ZH, Gomez-Sanchez E, Weiss RM & Felder RB (2008). Does aldosterone upregulate the brain renin-angiotensin system in rats with heart failure? *Hypertension* **51**, 727–733.

Zhang ZH, Yu Y, Kang YM, Wei SG & Felder RB (2008). Aldosterone acts centrally to increase brain renin-angiotensin system activity and oxidative stress in normal rats. *Am J Physiol Heart Circ Physiol* **294**, H1067–H1074.

Additional information

Competing interests

None.

© 2013 The Authors. The Journal of Physiology © 2013 The Physiological Society

Author contributions

G.C.B., K.B., J.B.A., E.G., J.E.R. and W.J.K. contributed to the collection, analysis and interpretation of data, and drafting and revising the manuscript. E.B. contributed to the conception and design of the experiments, collection, analysis and interpretation of data, and drafting and revising the manuscript. All authors approved the final version of the manuscript. In vitro and in vivo experiments were carried out at Thomas Jefferson University and Temple University; synthesis of G-1 and G-36 was carried out at New Mexico State University.

Funding

This work was supported by NIH grants HL090804 (to E.B.), HL091096 and HL091799 (to J.E.R.) and CA127731 (to J.B.A.).

Acknowledgements

None.

© 2013 The Authors. The Journal of Physiology © 2013 The Physiological Society